Hydrolytic Activity of A $Fe^{III}Zn^{II}$ Complex toward Di(*p*-nitrophenyl) Phosphate: A Functional Model of Heterobimetallic Phosphodiestelase

Hironobu Machinaga, Kanako Matsufuji, Masaaki Ohba, Masahito Kodera,† and Hisashi Ōkawa*
Department of Chemistry, Faculty of Science, Kyushu University, Hakozaki, Higashi-ku, Fukuoka 812-8581
†*Department of Molecular Science and Technology, Doshisya University, Kyotanabe, Kyoto 610-0321*

(Received April 12, 2002; CL-020313)

A $Fe^{III}Zn^{III}$ complex, $[FeZn(L)(AcO)_3]BPh_4\cdot H_2O$, of 2-{*N*-[2-(dimethylamino)ethyl]iminomethyl}-6-[*N*,*N*-di(2-pyridylmethyl)aminomethyl]-4-methylphenolate (L^-) hydrolyses tri(*p*-nitrophenyl) phosphate (TNP) into di(*p*-nitrophenyl) phosphate (DNP^-) and DNP^- into mono(*p*-nitrophenyl) phosphate (MNP^{2-}) in aqueous DMF.

Bimetallic cores exist at the active sites of many metalloenzymes and play an essential role in biological systems.[1] Dinuclear Zn cores are found at the active sites of phosphoesterases.[1–4] It is known that phosphotriesterase has only two Zn ions at the active site[5] whereas phospholipase C[6] and P1 nuclease[7] have an additional Zn ion to hydrolyze phosphodiester. It is supposed that these phosphodiesterases require a trinuclear Zn core to bind a substrate at the dinuclear Zn unit and to provide the nucleophile (OH^- or water) on the third Zn center (Figure 1, A). Moreover, heterodinuclear FeZn core was recognized at the active sites of purple acid phosphatase[8] and human calcineurin[9] that facilitate the hydrolysis of phosphodiesters into phosphomonoesters. It is considered that these enzymes employ a FeZn core instead of trinuclear Zn core to accommodate a substrate in chelating mode on the Fe center and provide the nucleophile on the Zn center[10] (Figure 1, B). Here we report a FeZn complex that has a hydrolytic function relevant to phosphodiesterase.

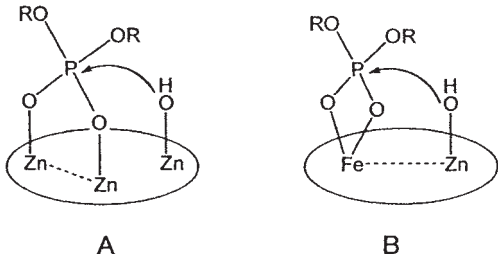

Figure 1. Supposed interation of phosphodiester with (A) triuclear Zn core and (B) dinuclear FeZn core in biological phosphodiester.

The FeZn complex $[FeZn(L)(AcO)_3]BPh_4\cdot H_2O$ of the end-off compartmental ligand HL (Fig. 2) was prepared as reddish brown crystals by the reaction of HL with $Fe(AcO)_3$ and $Zn(AcO)_2\cdot 2H_2O$ in methanol in the presence of sodium tetraphenylborate.[11]

The crystal structure of the FeZn complex was determined by single-crystal X-ray analysis.[12] An ORTEP view of the complex is shown in Fig. 2.[13] The two metal ions are bridged by the phenolic oxygen atom of L^- and two acetate groups in a '*syn-syn*' mode in the Fe–Zn separation of 3.385(1) Å. The Fe is bound to the bidentate arm and has a six-coordinate geometry together with two oxygen atoms (O2 and O4) from the bridging acetate groups and the oxygen atom (O6) from a unidentate acetate group. The Zn is bound to the tridentate arm and has a six-coordinate geometry together with two oxygen atoms (O3 and O5) from the bridging acetate groups. The average of the Fe-to-donor bond distances is 2.038 Å and the average of the Zn-to-donor distances is 2.123 Å. The site specificity of metal ions in the FeZn complex is in accord with our recent finding that a smaller metal ion is bound to the bidentate arm and a larger metal ion to the tridentate arm.[14]

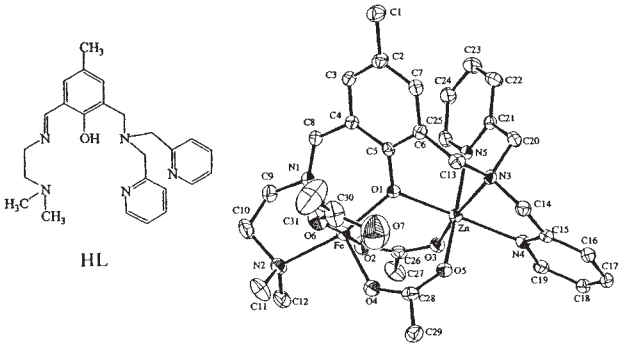

Figure 2. Crystal structure of $[FeZn(L)(AcO)_3]BPh_4\cdot H_2O$.

The complex shows two absorption bands at 340 nm (ε: 5500 $M^{-1}cm^{-1}$) and 480 nm (ε: 1000 $M^{-1}cm^{-1}$) in DMF. The spectrum is virtually invariant at a moderate complex concentration (1.0×10^{-3}–2.0×10^{-4} M). FAB mass spectrometry in *m*-nitrobenzylalcohol matrix indicated the parent ion peaks centered around m/z 654.2 corresponding to $\{FeZn(L)(AcO)_2\}^+$.

Hydrolytic activity of the FeZn complex toward tri(*p*-nitrophenyl) phosphate (TNP) and hydrogen di(*p*-nitrophenyl) phosphate (HDNP) was examined in aqueous DMF (H_2O : DMF = 2 : 98 in volume) at 25 °C by means of UV-visible spectroscopy. An aqueous DMF solution containing the FeZn complex (2.0×10^{-4} M) and the substrate (TNP or HDNP; 6.7×10^{-5} M) was prepared and subjected to spectroscopic measurements, using a complex solution in aqueous DMF (2.0×10^{-4} M) as reference.

Spectral changes in the hydrolysis of TNP by the FeZn complex are shown in Figure 3. The absorption band of TNP at 280 nm decreased with time with a concomitant increase at 304 nm due to the formation of DNP^-. Another absorption band observed at 422 nm is characteristic of *p*-nitrophenolate ion. Based on the absorbance at 304 nm, the hydrolysis of TNP into DNP^- must be completed in 100 min, but the absorbance at 304 nm, and that at 422 nm as well, showed a tendency to increase further. This fact suggests that the hydrolysis of BNP^- into MNP^{2-} occurs after the completion of the hydrolysis of TNP into

BNP^-. It is worth noting that the FeCu complex has a high activity in the hydrolysis of TNP relative to analogous ZnZn complex $[Zn_2(L)(AcO)_2]ClO_4$ when compared under the same conditions (see Insert).

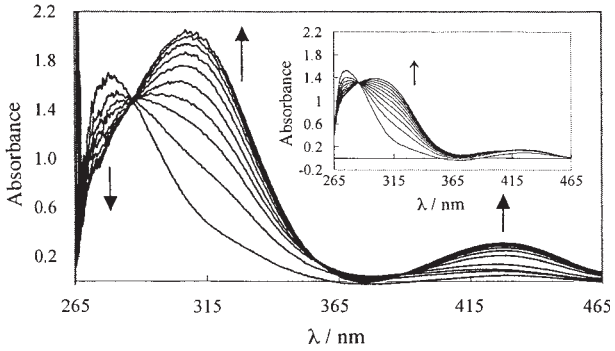

Figure 3. Spectral changes in the hydrolysis of TNP by the FeZn complex (measured every 10 minutes). The insert is the spectral changes in the hdrolysis of TNP by $[Zn_2(L)(AcO)_2]$-ClO_4 (measured every 10 minutes).

The hydrolysis of HDNP by the FeZn complex was studied by a separate run (Figure 4). In this case spectral changes in the near UV region are small because the absorption band of HDNP and that of MNP^{2-} are located at close wavelength (304 and 308 nm, respectively). However, the hydrolysis of HDNP by the FeZn complex is evident from the absorption band of *p*-nitrophenolate ion appearing at 425 nm. The solution soon after dissolution gave spectrum **a** which changed to spectrum **b** after 100 min and then gradually to **c** after 700 min. The spectral feature of **b** showing 'negative absorption' around 370 nm implies that a FeZn-DNP adduct is formed at the initial stage and the bound DNP^- is slowly hydrolyzed into MNP^{2-}. The hydrolysis of DNP^- into BNP^{2-} is almost completed in 700 min judged from the time-course of the absorbance at 425 nm.

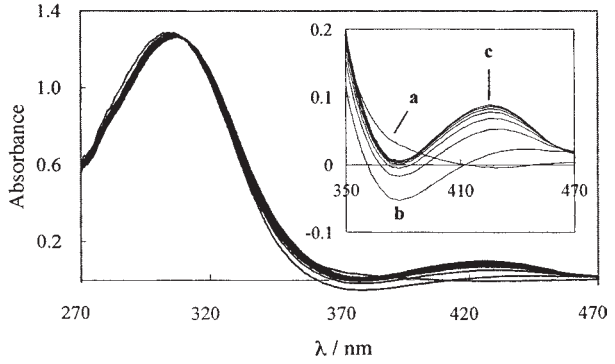

Figure 4. Spectral changes in the hydrolysis of DNP^- by the FeZn complex (measured every 100 minutes).

It must be emphasized that analogous ZnZn complex has no activity to hydrolyze DNP^-.[15] We have confirmed that the absorption bands at 340 and 480 nm of the FeZn complex in aq. DMF (H_2O : DMF = 2 : 98) diminish their intensities upon high dilution ($<2 \times 10^{-4}$ M). Furthermore, the molar conductance of the complex in aq. DMF increased upon dilution from 50 S cm^{2}mol^{-1} at 2×10^{-4} M to 90 S cm^{2}mol^{-1} at 4×10^{-5} M. These facts imply that one acetate bridge of $[FeZn(L)(AcO)_2]^{2+}$ is released more or less in a dilute solution, providing two vacant sites on the Fe center and one vacant site on the Zn center. The resulting $[FeZn(L)(AcO)]^{3+}$ can accommodate DNP^- in the chelating mode on the Fe center and OH^- (or H_2O) on the Zn center (Fig. 1, B), allowing the nucleophilic attack of the OH^- (or H_2O) to the phosphorus nucleus of DNP^-.

This work was supported by a Grant-in-Aid for COE Research 'Design and Control of Advanced Molecular Assembly System' (No. 08CE2005) and a Grant-in-Aid for Scientific Research Program (No. 13640561) from the Ministry of Education, Culture, Sports, Science and Technology.

References and Notes

1 D. E. Fenton and H. Ōkawa, "Perspectives on Bioinorganic Chemistry," JAI Press, London (1993), Vol. 2, p 81.
2 K. D. Karlin, *Science*, **261**, 701 (1993).
3 D. E. Wilcox, *Chem. Rev.*, **96**, 243 (1996).
4 G. C. Dismukes, *Chem. Rev.*, **96**, 2357 (1996).
5 J. L. Vanhooke, M. M. Benning, F. M. Raushel, and H. M. Holden, *Biochemistry*, **35**, 6020 (1996).
6 E. Hough, L. K. Hansen, B. Birkness, K. Jynge, S. Hansen, A. Hardvik, C. Little, E. J. Dodson, and Z. Derewenda, *Nature*, **338**, 357 (1989).
7 A. Lahm, S. Volbeda, F. Sakijama, and D. Suck, *J. Mol. Biol.*, **215**, 207 (1990).
8 N. Strater, T. Klabunde, P. Tucker, H. Witzel, and B. Krebs, *Science*, **268**, 1489 (1995).
9 C. R. Kissinger, H. E. Parge, D. R. Knighton, C. T. Lewis, L. A. Pelletier, A. Tempczyk, V. J. Kalish, K. D. Tucker, R. E. Showalter, E. W. Moomaw, L. N. Gastinel, N. Habuka, X. Chen, F. Maldonado, J. E. Barker, R. Bacquet, and E. Villafranca, *Nature*, **378**, 641 (1995).
10 K. Arimura, M. Ohba, T. Yokoyama, and H. Ōkawa, *Chem. Lett.*, **2001**, 1134.
11 Found: C, 63.14; H, 5.95; N, 6.69; Fe, 5.48; Zn, 6.17%. Clcd for $BC_{55}FeH_{61}N_5O_8Zn$: C, 62.78; H, 5.84; N, 6.66; Fe, 5.31; Zn, 6.21%.
12 Crystal data: $[FeZn(L)(AcO)_3]BPh_4 \cdot H_2O$, F.W. 1052.15; monoclinic space group $P2_1/n$(#14), $a = 18.8620(4)$, $b = 15.3948(4)$, $c = 20.0449(4)$ Å, $\beta = 117.222(1)°$, $V = 5157.9(2)$ Å^3, $Z = 4$, $D_c = 1.350$ g/cm^3. Intensity data were collected at −90 °C on a Rigaku RAXIS-RAPID Imaging Plate using graphite-monochromated Mo Kα radiation (μ(Mo Kα) = 8.02 cm^{-1}). No. of measured = 44600 and No. of unique reflections = 11633. R = 0.110 (all data), R_W = 0.159, R1 = 0.065 ($I > 2.00\sigma(I)$).
13 Fe–O1 1.970(3), Fe–O2 2.036(3), Fe–O4 1.949(3), Fe–O6 1.955(3), Fe–N1 2.086(4), Fe–N2 2.230(4), Zn–O1 2.092(3), Zn–O3 2.009(3), Zn–O5 2.144(3), Zn–N3 2.191(3), Zn–N4 2.131(3), Zn–N5 2.171(3) Å; Fe–O1–Zn 112.9(1), O1–Fe–O2 92.7(1), O1–Fe–O4 99.9(1), O1–Fe–O6 91.6(1), O1–Fe–N1 86.1(1), O1–Fe–N2 166.6(1), O2–Fe–O4 90.8(1), O2–Fe–O6 172.4(1), O2–Fe–N1 84.9(1), O2–Fe–N2 87.3(1), O2–Fe–O6 94.7(2), O4–Fe–N1 172.8(1), O4–Fe–N2 93.5(1), O6–Fe–N1 89.1(2), O6–Fe–N2 87.1(1), N1–Fe–N2 80.5(1), O1–Zn–O3 101.0(1), O1–Zn–O5 86.1(1), O1–Zn–N3 90.2(1), O1–Zn–N4 163.1(1), O1–Zn–N5 88.4(1), O3–Zn–O5 98.8(1),O3–Zn–N3, 164.8(1), O3–Zn–N4 93.6(1), O3–Zn–N5 91.5(1), O5–Zn–N3 92.3(1), O5–Zn–N4 83.3(1), O5–Zn–N5 169.1(1), N3–Zn–N4 77.2(1), N3–Zn–N5 78.4(1), N4–Zn–N5 99.7(1)°.
14 K. Abe, K. Matsufuji, M. Ohba, and H. Ōkawa, *Inorg. Chem.*, in press.
15 K. Abe, J. Izumi, M. Ohba, T. Yokoyama, and H. Ōkawa, *Bull. Chem. Soc. Jpn.*, **74**, 85 (2001).